The Journal of Neuroscience, November 15, 2000, 20(22):8452–8461

Neurotensin-Induced Bursting of Cholinergic Basal Forebrain Neurons Promotes γ and θ Cortical Activity Together with Waking and Paradoxical Sleep

Edmund G. Cape, Ian D. Manns, Angel Alonso, Alain Beaudet, and Barbara E. Jones

Department of Neurology and Neurosurgery, McGill University, Montreal Neurological Institute, Montreal, Quebec, Canada H3A 2B4

Cholinergic basal forebrain neurons have long been thought to play an important role in cortical activation and behavioral state, yet the precise way in which they influence these processes has yet to be fully understood. Here, we have examined the effects on the electroencephalogram (EEG) and sleep–wake state of basal forebrain administration of neurotensin (NT), a neuropeptide that has been shown *in vitro* to potently and selectively modulate the cholinergic cells. Microinjection of (0.1–3.0 mM) NT into the basal forebrain of freely moving, naturally waking-sleeping rats produced a dose-dependent decrease in δ (~1–4 Hz) and increase in both θ (~4–9 Hz) and high-frequency γ activity (30–60 Hz) across cortical, areas with no increase in the electromyogram. These EEG changes were accompanied by concomitant decreases in slow wave sleep (SWS) and transitional SWS (tSWS), increases in wake, and most remarkably, increases in paradoxical sleep (PS) and transitional PS (tPS), despite the virtual absence of SWS. The effects were attributed to direct action on cholinergic neurons as evidenced by selective internalization of a fluorescent ligand, Fluo-NT, in choline acetyltransferase (ChAT)-immunoreactive cells and stimulation by NT of bursting discharge in juxtacellularly recorded, Neurobiotin-labeled, ChAT-immunoreactive neurons. We conclude that NT-induced rhythmic bursting of cholinergic basal forebrain neurons stimulates rhythmic θ oscillations and γ across the cerebral cortex. With the selective action of NT on the cholinergic cells, their bursting discharge promotes θ and γ independent of motor activity and thereby also stimulates and enhances PS.

Key words: acetylcholine; choline acetyltransferase; EEG; sleep–wake states; slow wave sleep; δ

As the primary source of cholinergic innervation to the cerebral cortex (Lehmann et al., 1980; Rye et al., 1984), basal forebrain cholinergic neurons have been shown to play an important role in the modulation of cortical activity with behavioral state. Although lesions of the basal forebrain cause a decrease in cortical acetylcholine (ACh) release and cortical activation (LoConte et al., 1982), stimulation causes an increase in cortical ACh release and cortical activation (Casamenti et al., 1986). During the natural sleep–waking cycle, ACh release is higher during waking and paradoxical sleep (PS), when cortical activation occurs, than during slow wave sleep (SWS) (Celesia and Jasper, 1966; Jasper and Tessier, 1971).

In the study of the discharge patterns of the cholinergic basal forebrain neurons that would determine the way in which they modulate the cerebral cortex, it was recently found that identified cholinergic cells discharge *in vivo* in high-frequency bursts (Manns et al., 2000), in a manner similar to that originally described *in vitro* and shown to be dependent on intrinsic calcium currents (Khateb et al., 1992). The bursting discharge in the anesthetized animal occurs rhythmically in association with cortical activation and cross-correlated with cortical rhythmic θ-like activity. Such rhythmic discharge must depend on afferent input that would promote intrinsic rhythmic activity in the cholinergic cells. Indeed, NMDA, which was shown to induce rhythmic bursting in basal forebrain cholinergic cells *in vitro* (Khateb et al., 1995), was found when administered *in vivo* to freely moving rats to stimulate enhanced θ (4–9 Hz) and γ (30–60 Hz) electroencephalogram (EEG) activity together with an active waking state (Cape and Jones, 2000). However, NMDA is not selective in its action on cholinergic cells and would excite other noncholinergic, including GABAergic, cortically and caudally projecting neurons (Gritti et al., 1994, 1997).

Contained in brainstem and forebrain afferents to the basal forebrain (Morin et al., 1996; Morin and Beaudet, 1998), neurotensin (NT) appears to be unique in its capacity to modulate cholinergic basal forebrain neurons in a highly selective manner. In autoradiographic binding studies, the high-affinity receptor for NT (NT1) was found to be present in 95% of cholinergic (acetylcholinesterase reactive) neurons and not in noncholinergic neurons (Szigethy and Beaudet, 1987; Szigethy et al., 1990). Furthermore, a fluorescent analog of NT, Fluo-NT, was found to be internalized in a receptor-dependent manner within choline acetyltransferase (ChAT)-immunoreactive neurons (Alonso et al., 1994; Faure et al., 1995). In the same brain slices, NT was found to excite cholinergic, and not noncholinergic, neurons and to stimulate the cholinergic neurons to discharge in rhythmic bursts (Alonso et al., 1994).

In the present study, we administered NT by local microinjection into the basal forebrain of freely moving, naturally waking–sleeping rats to examine the effect of NT's excitation of cholinergic neurons on cortical activity and sleep–wake state. We also examined whether in the same animals a fluorescent analog of the peptide, Fluo-NT, was internalized by ChAT-immunoreactive neurons, and whether in urethane-anesthetized animals NT induced a bursting discharge in juxtacellularly recorded and Neurobiotin (Nb)-labeled ChAT-immunoreactive cells.

MATERIALS AND METHODS

Animals and surgery. Microinjections were performed in 22 male Wistar rats (200–215 gm, Charles River, St. Constant, Quebec, Canada) or when combined with single unit recording (see below) in seven male Long–Evans rats (200–250 gm, Charles River). All procedures were performed in accordance with the McGill University Animal Care Committee and the Canadian Council on Animal Care.

Received May 11, 2000; revised Aug. 23, 2000; accepted Aug. 24, 2000.

This research was supported by a grant from the Canadian Medical Research Council to B.E.J. E.G.C. was supported as a graduate student by the Fonds de Recherche en Santé du Québec (FRSQ), Réseau de Santé Mentale, Axe Sommeil et Vigilance, and I.M. was supported as a graduate student by the National Science and Engineering Research Council of Canada (NSERC). We thank Advanced Bioconcept (Montreal, Quebec, Canada) for donation of the Fluo-NT. We thank Dominique Nouel, Thomas Stroh, and Lynda Mainville for their contributions to this work.

Correspondence should be addressed to Dr. Barbara E. Jones, Montreal Neurological Institute, 3801 University Street, Montreal, Quebec, Canada H3A 2B4. E-mail: mcbj@musica.mcgill.ca.

Chronic experiments involving microinjections of NT or Fluo-NT in freely moving animals were performed in 16 (of the 22) Wistar rats. The rats were operated under barbiturate anesthesia (Somnotol, 67 mg/kg, i.p.) for stereotaxic implantation of indwelling guide cannulae and EEG and electromyogram (EMG) electrodes, as described previously (Cape and Jones, 1998). Field potential recordings were also performed in some animals (4 of the 16 that were used in the main and dose–response studies below) with deep electrodes in the hippocampus [−4.0 mm anteroposterior (AP), 2.2 mm lateral (L), −3.5 mm ventral (V) relative to bregma] and entorhinal cortex (−7.6 mm AP, 5.2 mm L, −7.2 mm V relative to bregma). Rats were maintained in recording chambers on a 12 hr light/dark cycle with food and water available *ad libitum*.

Acute experiments involving microinjections of Fluo-NT were performed in anesthetized animals (Somnotol, 67 mg/kg, i.p., using 6 of the 22 Wistar rats; see below). Those involving unit recording with microinjections were also performed in anesthetized animals (urethane, 1.4 gm/kg, i.p., using seven Long–Evans rats; see below).

Microinjections of NT. In chronic experiments involving microinjections of NT (in 12 of the 16 rats), the Ringer's and NT microinjections were performed in several stages (see Fig. 1) by use of a remotely controlled device as described previously (Cape and Jones, 1998). They were performed bilaterally in a volume of 0.5 μl solution per side and were delivered using 1 μl syringes, which were driven simultaneously by one syringe pump. In pilot experiments, previously published concentrations (1.0, 2.0, and 3.0 mM) of NT (Faure et al., 1995) were tested (in 3 of the 12 rats) before selection of 1 mM concentration of NT that was used for the main series of experiments (in 11 rats, including the 3 used in pilot experiments plus 8 other rats). Complete dose–response series were performed (in four rats, including three of the previous eight from the main series plus one other rat) by repeated trials using concentrations of 0 (Ringer's), 0.10, 0.25, 1.00, and 3.00 mM. Doses were administered in randomized order and separated by a minimum interval of 48 hr. Antagonism of the NT effect was tested in repeated trials (in three of the previous four rats in dose–response series) using atropine (30 mg/kg, i.p.) that was administered at the time of insertion of the inner cannulae, at ~30 min before the microinjection of (0.25 mM) NT.

Microinjection of Fluo-NT. Fluo-NT was administered in chronic experiments at a concentration of 0.25 mM in the same way as NT (above) in (4 of the 16) freely moving rats. Acute pilot experiments were performed (in three of the six) anesthetized rats (Somnotol, 67 mg/kg, i.p.) to test different concentrations (1.0, 0.50, and 0.10 mM) of Fluo-NT for the adequacy of fluorescent labeling. The fluoresceinylated derivative of NT, Fluo-NT, was kindly supplied by Advanced Bioconcept (Montreal, Quebec, Canada). It was dissolved together with a peptidase inhibitor, kelatorphan (15 mg/ml), in Ringer's solution.

The specificity of the Fluo-NT labeling was tested in acute experiments in three of the six anesthetized animals (Somnotol, 67 mg/kg, i.p.) by administration of (0.22 mM) Fluo-NT bilaterally and excess unlabeled (1.3 mM) NT unilaterally.

EEG recording and analysis. In the chronic experiments ($n = 16$), signals were recorded using a Grass model 78D polygraph and sent to a computer for digitization, storage, and subsequent analysis using Stellate Systems software (Montreal, Quebec). Behaviors were simultaneously observed using a video camera and scored on the record as annotations according to set categories, as described previously (Maloney et al., 1997; Cape and Jones, 1998). Recording was performed before and after microinjections during the period of ~11:00 A.M. to 3:00 P.M.

Each record was scored off-line by visual assessment for classification of 20 sec epochs according to sleep–wake state. The EEG and EMG activities were considered together with the behavioral annotations for scoring as wake (W), transition into SWS (tSWS), SWS, transition into PS (tPS) or PS (Maloney et al., 1997). Spectra were computed using Stellate Systems software by fast Fourier transform (FFT) based on 512 points for 2 sec epochs (or 256 samples per second) with a resolution of 0.5 Hz and a range of 1.5–63.5 Hz. Frequency bands were set as δ (1.5–4.0 Hz), θ (4.5–8.5 Hz), σ (9.0–14.0 Hz), β1 (14.5–18.5 Hz), β2 (19:0–30.0 Hz), and γ (30.5–58.0 Hz). On the basis of visually scored records, sleep–wake hypnograms were displayed in association with EEG frequency band activities for 20 sec epochs and data acquired from these files for the 30 min post-injection period using Eclipse software (Stellate Systems). Spectral analysis was also performed on 4 sec epochs for analysis of peak frequencies in association with band amplitudes using Rhythm software (Stellate Systems). Spectrum and frequency band activities were displayed and reported in analog-to-digital (A/D) converted amplitude units. The ratio of θ/δ was calculated and reported as a measure of θ activity in the EEG (Maloney et al., 1997). EMG amplitude was computed for the total spectrum up to 58.0 Hz. The EEG and EMG data for the figures were plotted with Origin (v5.0, Microcal Software, Northampton, MA).

Based on examination of EEG records and hypnograms from all animals, data from 2 of 16 rats in the chronic series were eliminated from the study because of the presence of seizure activity that is not uncommon in Wistar rats and emerged here after NT microinjections. These two rats had been used in the main series of NT microinjections ($n = 11$, thus reduced to 9). For all other rats, average EEG and state data for the post-injection period were analyzed by paired t test or ANOVA using repeated measures (or grouping by rat) depending on the specific experiment, as specified in Tables and Figure legends. Statistical comparisons of γ, δ, and θ/δ EEG activity and EMG activity, which have been shown to vary significantly as a function of behavior and state (Maloney et al., 1997), were performed. All statistics were performed using Systat (v9.0) software (Evanston, IL).

Unit recording and labeling. For combined unit recording and microinjections, acute experiments were performed on seven male Long–Evans rats, which were anesthetized (urethane, 1.4 gm/kg) and held in a stereotaxic frame. Microinjections in these experiments were performed unilaterally on the same side as the single unit recording. Adequate anesthesia was confirmed by the lack of hindlimb withdrawal in response to pinch, and additional anesthetic (0.1–0.15 gm/kg) was administered if withdrawal occurred. Body temperature was thermostatically maintained above ~35°C with a heating pad. Juxtacellular recording and labeling of cells with Nb (Vector Laboratories, Burlingame, CA) was performed using an intracellular amplifier (IR-283; Neuro Data Instruments, New York, NY) as described previously (Pinault, 1996; Manns et al., 2000). EEG was also recorded from retrosplenial cortex and prefrontal cortex. Unit discharge was examined before, immediately after, and during the maximal effect of NT microinjection. Using 1 min epochs of stationary data, the average discharge rate was calculated from the peristimulus histogram (PSH), the predominant instantaneous firing frequency was determined from the first-order interspike interval histogram (ISIH), and the presence of rhythmic unit and unit-to-EEG cross-correlated discharge was assessed by autocorrelation histogram (ACH) and spike-triggered averaging (STA), as described previously (Manns et al., 2000). On the basis of the properties of unit discharge and the immunostaining of the Nb-labeled cells for ChAT (see below), data from cholinergic cells ($n = 3$) were selected for detailed analysis and presentation.

Immunohistochemistry. At the conclusion of the chronic experiments, animals were killed with a lethal dose of pentobarbital (Somnotol, ~120 mg/kg, i.p.) and perfused through the heart with a fixative solution [3.0% paraformaldehyde, as published previously (Gritti et al., 1997)]. In both chronic and acute experiments involving microinjections of Fluo-NT, animals were killed 15 min after the microinjection by perfusion. In acute experiments involving unit recording and microinjection, the urethane-anesthetized animals were killed by perfusion after completion of the microinjection and subsequent juxtacellular labeling of the recorded unit.

In animals having received microinjections of NT, brains were processed for ChAT immunostaining to examine the injection sites in relation to the cholinergic cells. Immunohistochemistry was performed using the peroxidase–antiperoxidase (PAP) technique as published previously (Gritti et al., 1997). Sections were incubated overnight with rabbit anti-ChAT antiserum (1:3000; Chemicon International, Temecula, CA) followed by donkey anti-rabbit secondary antisera and rabbit PAP antibodies (Jackson ImmunoResearch Laboratories, West Grove, PA) and revelation with

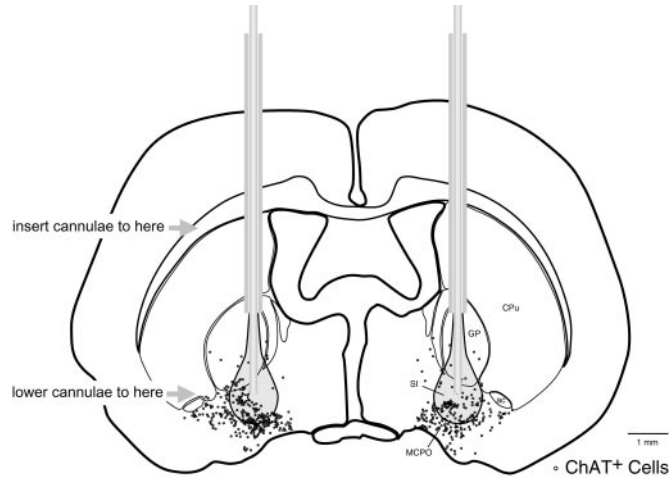

Figure 1. Schematic atlas section through the basal forebrain showing the location of the microinjection cannulae (based on visible tracks) in relationship to ChAT-immunoreactive neurons. Inner cannulae filled with Ringer's or NT were first inserted into indwelling guide cannulae (to within ~2 mm of tip as indicated), where they were held until the time of injection. Immediately before injection, inner cannulae on both sides were lowered by a remote driving mechanism to pass out of the guide cannulae to the injection site (~2 mm below guide cannulae as indicated) in the SI and above the MCPO. The representation of the injected fluid is based on estimates previously established with neuroanatomical tracers. In this area and beyond within the SI and MCPO, punctate fluorescent labeling was visible with injections of Fluo-NT within ChAT-immunoreactive cells (see Fig. 7*A–D*). Also within the SI and MCPO, cells (*stars* on *left* side) that were juxtacellularly recorded and labeled with Nb during NT microinjections in anesthetized animals were identified as ChAT-immunoreactive (see Fig. 7*E–H*). *ac*, Anterior commissure; *CPu*, caudate putamen; *GP*, globus pallidus; *MCPO*, magnocellular preoptic nucleus; *SI*, substantia innominata.

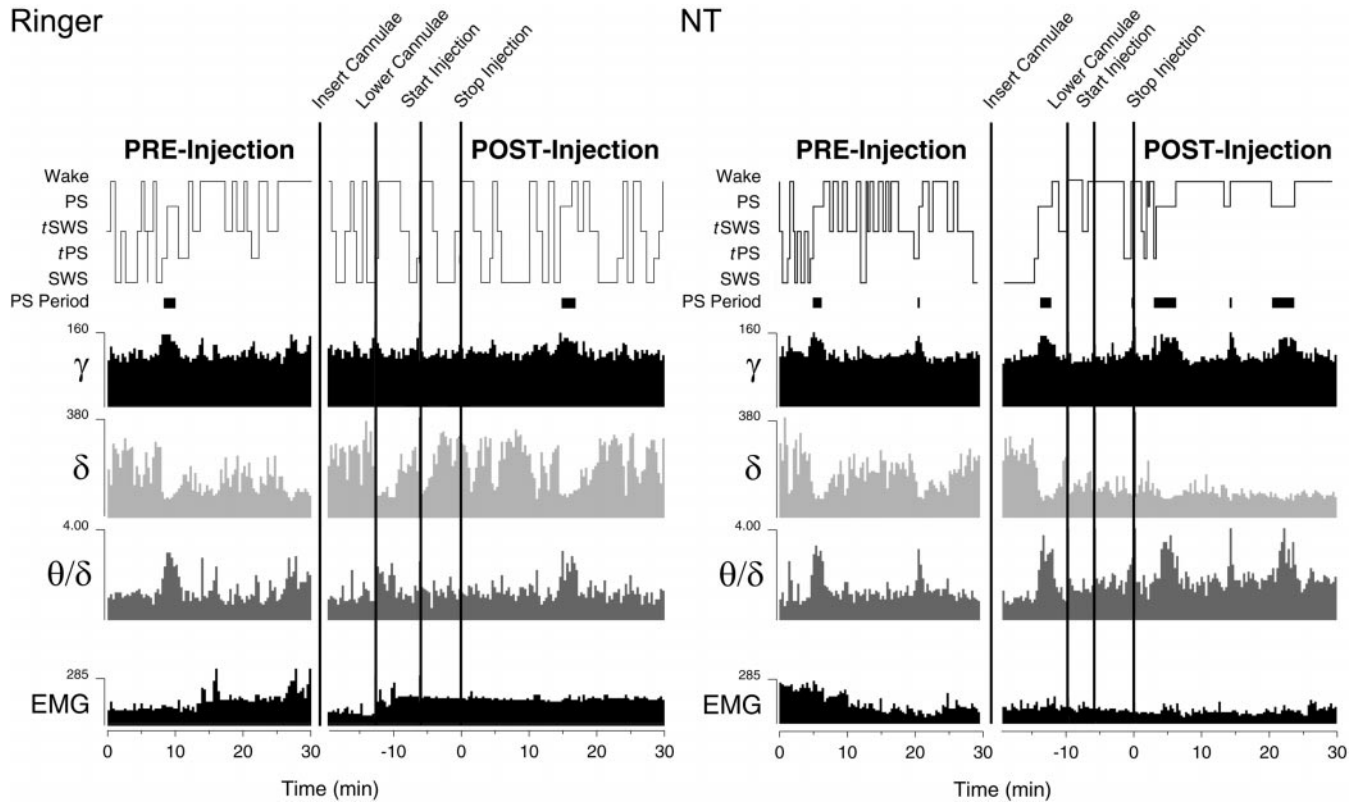

Figure 2. Hypnograms showing sleep–wake state changes in conjunction with EEG and EMG activity changes before and after injection of Ringer's (*left*) and NT (*right*, rat B11). After insertion of the Ringer's- or NT-filled cannulae into the indwelling cannulae (Fig. 1) and resumption of sleeping by the animal, recording was resumed, and the filled cannulae were lowered into the tissue for injection ~2 min later that lasted ~5 min (Fig. 1). Note that during and after the entire microinjection procedure, Ringer's does not appear to disrupt the sleep–wake cycle and associated EEG activity. In contrast, NT markedly changes the cycle and EEG from the moment the filled cannulae are lowered into the tissue and for the duration of the injection and post-injection period. After NT, δ is diminished, and SWS is absent. θ becomes relatively high and together with γ increases in association with the occurrence of PS directly after waking in the absence of SWS. Sleep–wake states were scored off-line by visual assessment of the record together with behavioral annotations. The EEG is from the right retrosplenial lead and shows band activities for γ (30–58 Hz), δ (1.5–4 Hz), and θ (θ/δ: 4.5–8.5 Hz/1.5–4 Hz); EMG is from the neck muscles (1–58 Hz). Each activity is scaled to maximum and reported in AD units (where for EEG 100 μV ≅ 125 AD units) for 20 sec epochs.

Table 1. Relative EEG activity and time spent in sleep–wake states during the 30 min post-injection period after Ringer's and (1 mM) NT[a]

	Drug trials		
	Ringer's	(1.0 mM) NT	Statistic[a] (p)
Activity (total)			
γ	15.4 ± 0.9	18.7 ± 0.7	***
δ	21.8 ± 1.3	17.0 ± 0.8	***
θ/δ	1.10 ± 0.07	1.40 ± 0.07	***
EMG	308.5 ± 63.0	295.7 ± 51.5	
State			
Wake	26.5 ± 7.1	45.3 ± 8.4	*
tSWS	19.5 ± 2.9	11.9 ± 3.7	
SWS	39.8 ± 4.8	3.1 ± 1.8	***
tPS	9.9 ± 2.6	25.5 ± 7.0	*
PS	4.2 ± 1.0	14.2 ± 2.4	*

[a]Data are presented as mean ± SEM for repeated trials in nine rats comparing average values in Ringer's and NT conditions for 20 sec epochs. For EEG activity, γ and δ are presented as relative amplitude (% total amplitude), together with θ/δ ratio and EMG absolute amplitude (AD units). Statistics are based on Student's paired t test (*$p \leq 0.05$, ***$p \leq 0.001$). For % state, a repeated measures ANOVA was also performed to establish first a significant overall effect of drug (as repeated measure) by state (as grouping factor) and revealed a significant interaction between drug and state ($F = 18.2$; df = 1,40; $p = 0.000$).

diaminobenzidine. Cells were plotted using an image analysis system (Biocom, Paris, France).

In animals having received microinjections of Fluo-NT, 20-μm-thick frozen sections were cut and collected every 200 μm for processing. Half of the series was cold-mounted for simple visualization of the Fluo-NT fluorescence, and the other half was incubated with anti-ChAT antiserum for dual visualization of Fluo-NT and ChAT. The latter sections were free-floated at 4°C overnight in rabbit anti-ChAT antiserum (1:200) and then at room temperature for 2 hr in goat anti-rabbit Texas Red (1:50; Jackson).

Brains in which recorded units were labeled with Nb were processed for dual staining of Nb and ChAT. Frozen sections were cut (30 μm) and incubated overnight in rabbit anti-ChAT antiserum (1:3500) followed by incubation with Cy2-conjugated streptavidin (1:800; Jackson) to reveal Nb and with Cy3-conjugated donkey anti-rabbit antiserum (1:1000; Jackson) to reveal ChAT. Sections were then mounted and viewed by fluorescent microscopy using a Leitz Dialux microscope equipped with a Ploemopak 2 reflected light fluorescence illuminator with Leica filter cubes for fluorescein (I3) and rhodamine (N2.1).

Confocal microscopy. Sections were examined using a Zeiss confocal laser scanning microscope (CLSM 410) equipped with an Axiovert 100 inverted microscope and an argon/krypton laser. FITC signals for Fluo-NT were imaged by exciting samples with 488 nm light, and Texas Red for ChAT was imaged in the same sections by 568 nm light. Images were acquired sequentially as single transcellular optical sections and averaged over 32 scans per frame. Images, processed using the Carl Zeiss CLSM software (v3.1), were prepared for publication using Adobe Photoshop (v5.0, Adobe Systems, San Jose, CA).

RESULTS

The microinjection cannulae were symmetrically placed above the major population of basal forebrain cholinergic neurons as was evident by the tracks of the cannulae seen in relation to ChAT-immunostained cells in processed brains (Fig. 1). The tracks were evident passing through the caudate putamen and medial part of the globus pallidus and extending ventrally into the substantia innominata (SI) above the magnocellular preoptic nucleus (MCPO), where large numbers of ChAT-immunoreactive cells are located.

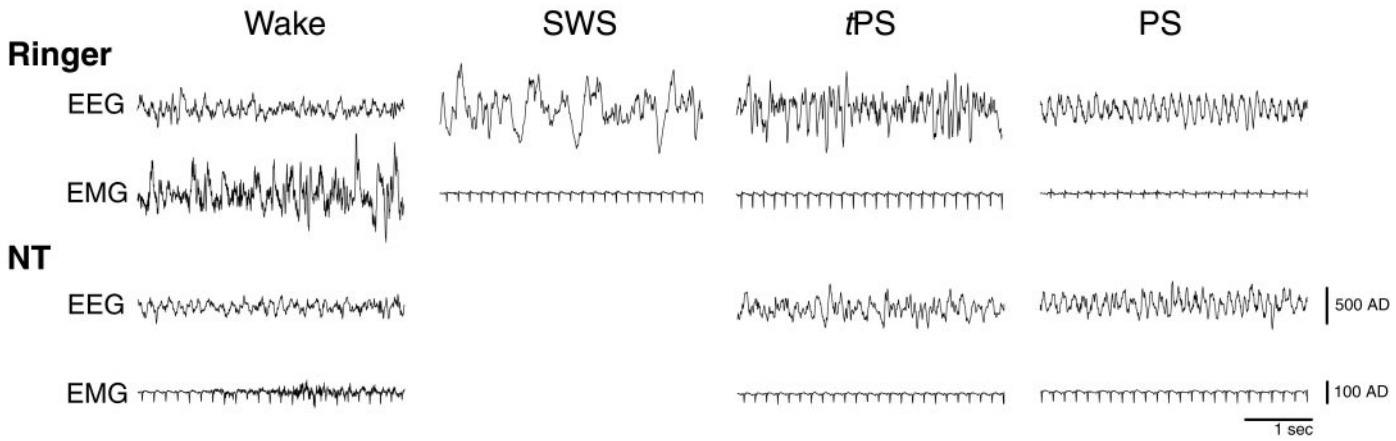

Figure 3. Sample recordings of EEG from retrosplenial cortex and EMG from neck muscles during states observed after *Ringer* (*top*) and *NT* (*bottom*). EMG also shows ECG activity when postural muscle tonus is low. Note the presence of θ activity with active waking after Ringer's and with quiet waking after NT (as evident by respective EMG signals), the absence of SWS after NT, the occurrence of tPS with a predominance of θ after NT, and the similar appearance of PS in both conditions. (Amplitudes shown as AD units are presented in Fig. 2.)

Effects of NT microinjections on EEG and sleep–wake states

Microinjections of (1.0 mM) NT into the basal forebrain altered the EEG and natural sleep–waking cycle of the rat ($n = 9$) (Fig. 2). From the moment the NT-filled cannulae were lowered into the tissue and through the injection and post-injection periods (Fig. 2*B*), δ activity was diminished and associated with a loss of SWS during the day, when rats are normally in SWS the majority of the time (Fig. 2*A*). In the absence of δ activity, θ activity was relatively high and associated with moderate γ activity. As judged from the EEG, EMG, and behavioral observations used in the visual scoring of sleep–wake states, a state of PS or tPS occurred in the absence of SWS and alternated directly with a state of wake. From the EMG amplitude, which usually remained low, it appeared that the animals remained quiet while awake as well as asleep after the NT. As confirmed in the behavioral annotations, the wake state after NT was predominantly quiet and characterized by a reclining, outstretched posture with head down. The passage into tPS or PS was usually marked only by closing of the eyes, with no other postural change. At one moment, the rat would be lying quietly with eyes open showing "quiet waking" behavior, and the next moment, without changing position, it would close its eyes and begin twitching, thus showing "sleeping with twitches" or PS behavior. All rats receiving (1.0 mM) NT (9 of 9) showed transitions from wake directly into PS or tPS with no intervening SWS or tSWS. Active behaviors, including moving and eating, which were accompanied by high EMG, were also seen occasionally after NT, because they occur normally during this period of the day (Maloney et al., 1997). A direct passage from these active or attentive waking behaviors to a PS-like state was never seen. None of the behaviors or postures appeared abnormal.

Across animals receiving (1.0 mM) NT, there was a significant decrease in relative δ band activity and a significant increase in relative γ band activity and θ/δ ratio as compared with Ringer's on the retrosplenial lead ($n = 9$) (Table 1). There was no significant change in EMG. Sleep–wake states were significantly altered in amount, with a significant decrease in SWS, significant increase in wake, and significant increase in PS and tPS. In one animal (B29), PS reached 23% and tPS reached 36%, representing together ~60% of total recording time. Within the individual states (except SWS because of the few epochs after NT), relative γ and δ, as well as θ/δ ratio, and EMG measures were not significantly different between the Ringer's and NT conditions across animals (for the 9 rats presented in Table 1, $p > 0.05$, according to paired t tests per state; data not shown). Varying according to behavior, wake epochs could be characterized by moderate θ with high EMG activity (associated with active waking) after Ringer's and NT, but they were also and most often characterized by moderate θ with low EMG activity (associated with quiet waking) after NT (Fig. 3; and see below). SWS was absent in most animals after NT and replaced predominantly by tPS leading to PS (Fig. 3; and below). As a transitional state (Maloney et al., 1997), tPS varied between a predominance of spindle activity accompanied by θ, which was most characteristic after Ringer's, to a predominance of θ accom-

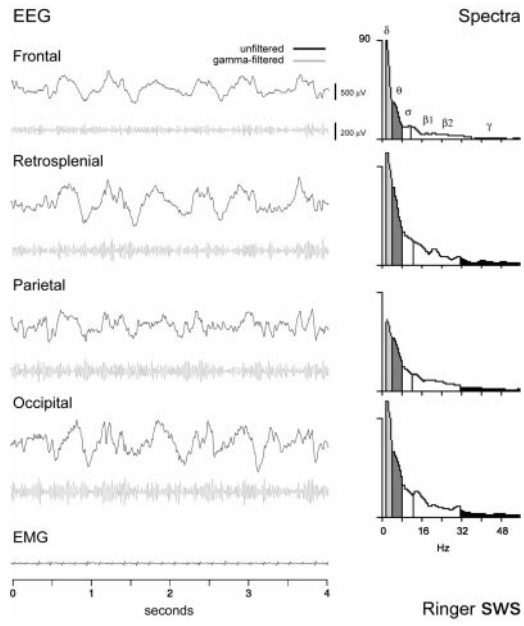

Figure 4. EEG record and spectral analysis after Ringer's microinjection (in rat B11). SWS was the predominant state after Ringer's and, like normal SWS, was characterized by a curled sleeping posture behaviorally and by high amplitude δ activity (evident in *top*, unfiltered *black traces*) and relatively low amplitude γ activity (evident in *bottom*, *gray traces* filtered for 30–58 Hz). These characteristics are evident in the spectra from the same 4 sec epochs (*right*), in which the predominant peak on all leads is in the δ band (2.0 Hz) and accompanied by a relatively low amplitude in the γ band. The EEG was recorded by reference to an electrode in the rostral frontal bone from the anterior medial frontal, retrosplenial, parietal, and occipital cortical regions (shown here for the right side). Voltage scales are the same for all cortical leads. (Note that the amplitude of the frontal lead is the lowest because of its proximity to the reference electrode.) EMG recorded from the neck muscles also shows ECG activity when postural muscle tonus is low, as here during sleep. Spectra are displayed in amplitude (*AD*) units (per 0.5 Hz; 100 μV ≅ 125 AD units). δ, θ, and γ frequency bands are differentially *shaded* (as in the hypnograms in Fig. 2); σ and β bands are *unshaded*.

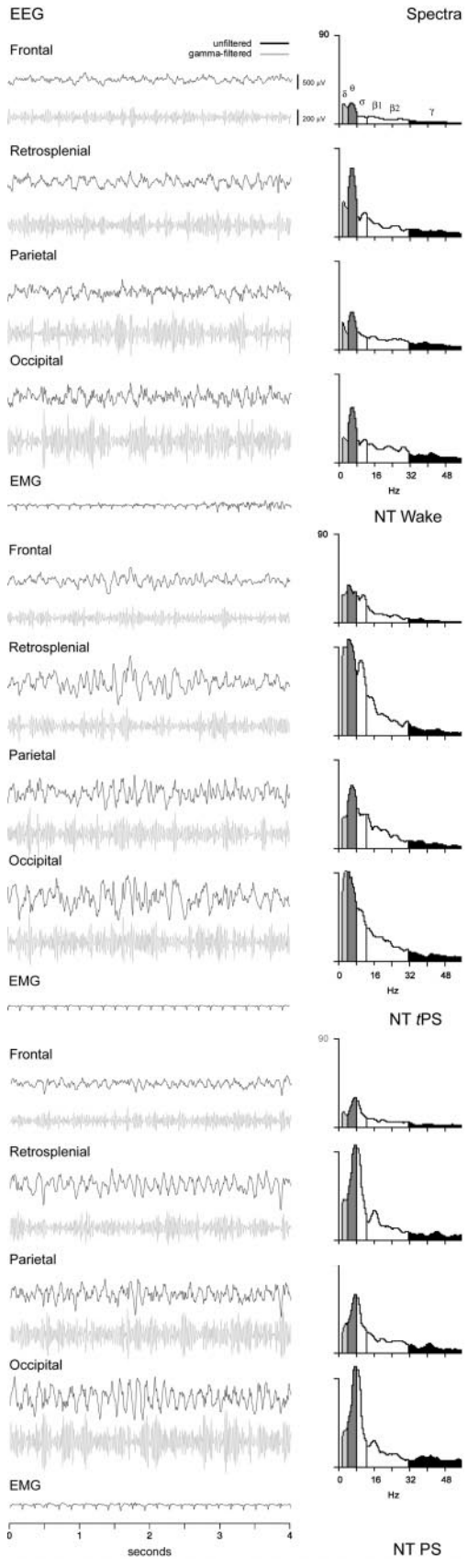

Figure 5. EEG records and spectral analyses after NT during waking (*top*), tPS (*middle*), and PS (*bottom*, in rat B11). The predominant state was wake and often characterized behaviorally (as during this epoch shown on *top*) by a quiet state and a reclining posture. The unfiltered EEG is dominated by the occurrence of rhythmic slow activity on all leads that corresponds to peaks in the θ band (~7.0–7.5 Hz) and moderately high amplitude γ activity. EMG was low, indicating postural muscle relaxation. A large

panied by spindle activity, which was most characteristic after NT (Fig. 3; and below). PS was similar in the two conditions (Fig. 3). As in baseline conditions (Maloney et al., 1997), EMG after Ringer's and NT was low throughout sleep [when the electrocardiogram (ECG) signal also becomes evident] (Fig. 3) and often slightly higher in PS because of the muscular twitches of whiskers, ears, and body musculature that are picked up on the electrodes in the neck muscles.

Although the predominant EEG activity after Ringer's was composed of δ activity (1.5–4 Hz) in association with SWS (Fig. 4), the predominant EEG activity after NT was composed of θ-like activity (4.5–8.5 Hz) in association with wake, tPS, or PS (Fig. 5*A–C*) on all cortical leads. In comparison with the Ringer's SWS δ activity, the NT θ-like activity was consistently associated with higher γ activity (30–58 Hz) (Figs. 3, 4). The EMG was low, indicative of postural muscle relaxation or atonia during the quiet waking, tPS, and PS states (Fig. 5). In spectra from 4 sec epochs sampled during the post-injection period (~4–12 min) during which the maximal, stable effect of NT was observed, the average low peak frequency was significantly higher across cortical areas after NT ($n = 5$) (Table 2). The average peak frequency shifted from the δ range into the θ range, although it differed in specific frequency across areas, being the highest on the retrosplenial and lowest on the frontal lead (Table 2). The differences in peak frequencies across areas appeared to be greatest during waking behaviors and tPS and the least during PS and SWS. In animals with deep electrodes in the hippocampus and entorhinal cortex ($n = 4$), θ activity was often evident on these leads when it was present on other cortical leads but would also differ in frequency and phase from that on the other cortical leads at particular moments of the different behavioral and sleep–wake states. There was no specific peak or shift in peak frequency in the γ band with NT, only an increase in the average amplitude of the entire band (Table 2).

Increasing doses of NT were associated with increasing γ amplitude and θ/δ ratio and decreasing δ amplitude with no systematic change in EMG ($n = 4$) (Fig. 6*A*). Paralleling the EEG changes were dose-dependent increases in wake and in PS, tPS and decreases in SWS, tSWS (Fig. 6*B*). PS and tPS increased in a linear manner up to a maximum with (1.0 mM) NT and represented together ~40% of recording time on average with that dose. Wake reached a maximum with (3.0 mM) NT, representing ~75% of recording time, at which dose, PS and tPS were similar in amount to Ringer's (<20%).

The changes in EEG induced by (0.25 mM) NT were largely antagonized with the systemic administration of atropine (30 mg/kg, i.p.) ($n = 3$) (Table 3). Microinjection of NT after atropine no longer produced an increase in γ or decrease in δ as it did before atropine (Table 3). The average θ/δ ratio was not increased by NT after atropine; however, the difference in the ratio between NT on the one hand and atropine and NT together with Ringer's on the other did not reach significance, and thus the statistical test of the

←

percentage of time was also spent in tPS, which often occurred directly after wake (as in the epoch shown in the *middle*), with the simple closing of the eyes while the rat remained in a reclining, uncurled posture. In this and similar epochs of tPS, the EEG is characterized by the presence of θ-like activity mixed with slower δ or spindle-like activity. The spectra reveal peaks at the border between δ and θ bands (~3.5–4.5 Hz) on frontal, retrosplenial, and occipital leads together with a secondary peak in the σ band (~10 Hz) reflecting spindle-like activity, and a peak in the middle of the θ band (6.0 Hz) on the parietal lead. γ band activity is high relative to SWS (Fig. 4). EMG indicates postural muscle atonia. Typical PS, which was behaviorally and electroencephalographically indistinguishable from normal PS, occurred a large percentage of the time after NT. In these cases (as for the epoch shown at the *bottom*), muscle twitches were evident while the animal was in a reclining, partially curled (or also fully curled) posture with eyes closed. The EMG shows evidence of small twitches during postural muscle atonia (when ECG signal is also evident). The unfiltered EEG is dominated by θ-like activity on all leads, with spectral peaks at the high end of the θ band (~8.0 Hz) and relatively high amplitude γ activity, as compared with Ringer's SWS (Fig. 3). See Figure 4 for details.

Table 2. EEG frequency peaks and band amplitudes obtained from spectral analysis of epochs from four cortical areas during the maximal, stable effect after (1.0 mM) NT as compared with Ringer's[a]

	Drug trials		ANCOVA					
	Ringer's	NT	Drug (*F*)	df	Area (*F*)	df	Drug × Area (*F*)	df
High peak frequency (30–60 Hz)		Mean ± SEM						
Avg	36.1 ± 0.3	36.3 ± 0.2	0.7	1	1.2	3	0.6	3
F	36.2 ± 0.7	35.8 ± 0.6						
RS	36.7 ± 0.5	36.4 ± 0.5						
P	36.0 ± 0.6	36.7 ± 0.5						
O	35.4 ± 0.9	35.9 ± 0.4						
Low peak frequency (1–10 Hz)								
Avg	3.1 ± 0.1	4.1 ± 0.2	19.51	1***	9.9	3***	1.0	3
F	2.4 ± 0.1	3.0 ± 0.3						
RS	3.2 ± 0.3	4.6 ± 0.3						
P	3.4 ± 0.2	4.2 ± 0.3						
O	3.3 ± 0.2	4.3 ± 0.3						
Band amplitude (AD)								
γ								
Avg	139.2 ± 3.5	145.9 ± 3.8	4.129	1*	325.0	3***	0.6	3
F	74.3 ± 1.8	81.0 ± 3.1						
RS	168.1 ± 3.6	170.7 ± 4.7						
P	143.0 ± 4.5	157.6 ± 7.1						
O	170.3 ± 4.8	174.4 ± 4.4						
δ								
Avg	224.7 ± 8.8	123.3 ± 4.6	117.8	1***	32.9	3***	0.2	3
F	149.3 ± 11.6	82.8 ± 6.5						
RS	281.1 ± 19.9	147.6 ± 9.7						
P	205.4 ± 8.7	121.0 ± 8.7						
O	263.0 ± 15.1	141.7 ± 8.2						
θ/δ								
Avg	1.02 ± 0.03	1.27 ± 0.03	39.04	1***	8.24	3***	1.01	3
F	0.89 ± 0.04	1.03 ± 0.04						
RS	1.06 ± 0.08	1.40 ± 0.08						
P	1.06 ± 0.05	1.25 ± 0.05						
O	1.08 ± 0.07	1.37 ± 0.08						
EMG								
Avg	326.7 ± 23.0	385.0 ± 26.5	2.86	1				

[a]Measures were taken from nine 4 sec epoch samples (at 1 min intervals from 4 to 12 min post-injection) from the four cortical areas (F, frontal; RS, retrosplenial; P, parietal; O, occipital) after Ringer's and NT in five rats. Statistics were performed on natural log (Ln) transformed values that were normally distributed. The average (Avg) values per drug condition and the individual values for each area per drug (mean and SEM) were calculated and reported from the raw values in Hz for frequency, in AD units for amplitude bands (100 μV ≅ 125 AD units) from EEG and EMG, or as the ratio of θ/δ. An analysis of covariance (ANCOVA) was performed with each EEG measure as the dependent variable, drug (2) and area (4) as the independent variables, and sample (9) and rat (5) as covariates (with $df_{error} = 349$). Significant main effects of drug (*$p < 0.05$; **$p \leq 0.01$; ***$p \leq 0.001$) were not associated with any significant interactions of drug with area, thus not calling for *post hoc* tests per area.

hypothesis that atropine completely antagonized the NT-induced increase in θ activity was not confirmed (Table 3). Atropine by itself, however, produced a continuous waking state during which, as also seen after the subsequent microinjection of NT, movement could occur and be accompanied by θ, even though δ activity was predominant. Nevertheless, atropine clearly prevented the NT-induced enhancement of tPS and PS during which θ was most prominent.

Labeling of cholinergic cells after Fluo-NT microinjections

To visualize NT's target cells, the fluorescent ligand, (0.25 mM) Fluo-NT, was administered bilaterally by microinjection to the freely moving, naturally waking–sleeping rats in the same manner as the nonfluorescent ligand (Fig. 1), except that its effects were examined for a post-injection period of 15 min to ensure that the ligand would be present in adequate amounts for histofluorescent visualization after rats were killed. In repeated trials ($n = 4$), (0.25 mM) Fluo-NT produced changes in EEG activity and sleep–wake states that did not differ from those after (0.25 mM) unlabeled NT during the 15 min post-injection period. Relative γ (21.1 ± 1.9%) and θ/δ ratio (1.75 ± 0.18) were similarly elevated, and relative δ (12.2 ± 1.4%) similarly decreased with the fluorescent as compared with the nonfluorescent NT (γ: 19.6 ± 1.41%; θ/δ: 1.78 ± 0.19%; δ: 12.1 ± 1.59%). Wake (41.7 ± 13.44%) and tPS+PS (28.9 ± 9.59%) were also as high after Fluo-NT, as after unlabeled NT (wake: 37.22 ± 11.45%; tPS+PS: 28.9 ± 11.33%).

In brains of animals having received microinjections of Fluo-NT ($n = 4$), evidence of fluorescent labeling was visible by light microscopy. A diffuse fluorescent staining of the cytoplasm of a small number of cells was evident in the immediate vicinity of the injection tracks. Beyond this region, very light and fine labeling was detectable in cells within the SI and MCPO. When examined by

confocal laser scanning microscopy, this fine fluorescent staining was seen to correspond to punctate labeling within the cytoplasm of neuronal perikarya (Fig. 7*A*,*C*). The punctate staining was evident predominantly in medium to large cells, which varied in shape from fusiform to polygonal. Such Fluo-NT+ cells were found within the SI and MCPO extending in a radius of up to 1 mm from the injection tracks and thus beyond the region that was estimated by volume of the solution as the immediate injection site (Fig. 1). In sections immunostained for ChAT, it appeared that although diffuse fluorescent labeling was present in ChAT-negative cells in the immediate vicinity of the tracks, the Fluo-NT punctate labeling was found within ChAT-positive neurons in the SI and MCPO (Fig. 7*B*,*D*).

In acute experiments in anesthetized rats ($n = 3$) that were aimed at testing the specificity of the Fluo-NT labeling, it was found that although diffuse labeling of neurons was still visible around the injection track, punctate Fluo-NT perikaryal labeling was no longer visible in neurons in the SI and MCPO on the side where excess unlabeled NT was injected in combination with the (0.22 mM) Fluo-NT.

Effects of NT microinjections on the discharge of cholinergic neurons

The effect of NT microinjection after the discharge of basal forebrain cholinergic units was examined in urethane-anesthetized animals. Each unit was labeled by juxtacellular application of Nb for subsequent histochemical processing and examination of ChAT immunoreactivity. Three units displayed discharge properties typical of cholinergic neurons according to previously established characteristics, notably the distinguished presence of rhythmic high-frequency burst discharge with somatic stimulation-induced cortical activation (Manns et al., 2000). Of these, two were successfully labeled with Nb (Fig. 7*E*,*G*), and both of these were found to be positive for ChAT immunostaining (Fig. 7*F*,*H*). One was located in the SI and the other in the MCPO (Fig. 1). These Nb+/ChAT+ neurons, as well as the electrophysiologically characterized cholinergic-like cell, all showed changes in their rate and pattern of discharge that were associated with changes in EEG activity after the NT microinjection as compared with the preinjection recording baseline (Fig. 8). All increased their average rate of discharge (according to PSH measures) and instantaneous firing frequency (according to ISIH measures) shortly after, if not before, the end of the NT microinjection (Fig. 8, *middle panel*). Additionally, they all showed high frequency bursts (>80 Hz) in their activity after NT that were infrequent preceding NT in the unstimulated condition (Fig. 8, *arrows*). In two cells, this bursting discharge became rhythmic spontaneously (Fig. 8, *SI*; and data not shown), and in the other cell, it did so with tail pinch (Fig. 8, *MCPO*, as evaluated by autocorrelation histogram measures) in parallel with the appearance of rhythmic slow activity on the EEG. The rhythmic burst discharge of all three was temporally cross-correlated with the retrosplenial and prefrontal EEG signals [as evaluated by STA, see Manns et al. (2000)]. The rhythmic discharge of the MCPO unit matched the predominant activity in the retrosplenial cortex, whereas that of the SI unit matched the slower predominant activity in the prefrontal cortex (as evident in spectral analysis).

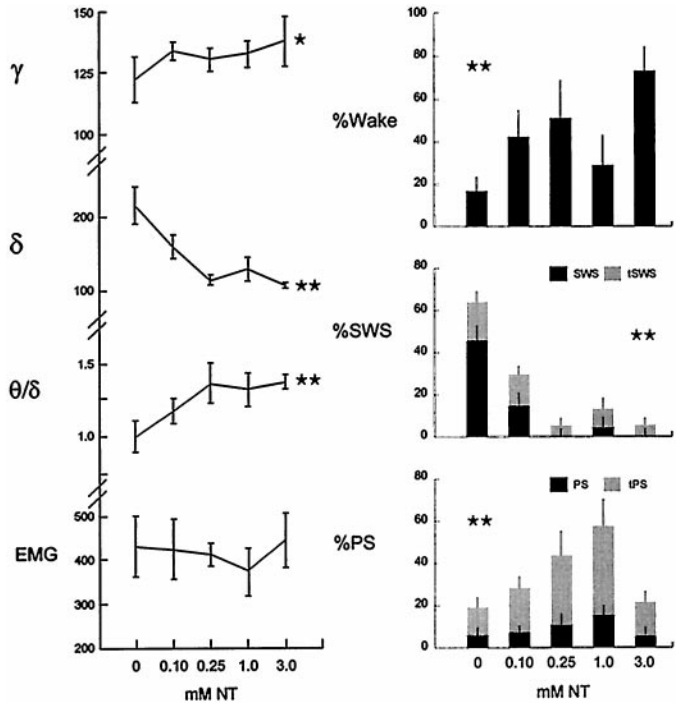

Figure 6. Changes in EEG activities (*left*) and sleep–wake state (*right*) as a function of the dose of NT. With increasing doses, γ and θ increased and δ activity decreased (*left*). γ and δ activities, as well as EMG, are presented, as average amplitude in AD units (100 μV ≅ 125 AD units) and θ as the ratio of θ/δ for 20 sec epochs during the 30 min post-injection period (mean ± SEM from 4 rats). Statistics were performed on natural log values that were normally distributed. The data were analyzed by ANOVA with dose as a repeated measure (performed with the metric 0, 0.1, 0.25, 1.0, and 3.0 mM) and *post hoc* polynomial contrasts for linear trend analysis (showing a significant trend for γ, according to the cubic polynomial: $F = 10.45$, df = 1,3, $p = 0.048$; for δ, according to the linear: $F = 47.25$, df = 1,3, $p = 0.006$; and for θ/δ, according to the quadratic: $F = 38.76$, df = 1,3, $p = 0.008$; $^{*}p < 0.05$; $^{**}p \leq 0.01$). Although wake and PS together with tPS increased as a function of dose, SWS together with tSWS decreased as a function of dose (*right*). State data (mean ± SEM from 4 rats) are presented as the percentage of the 30 min post-injection recording period. In an overall test, in which dose was examined across states (entered as a grouping factor with 5 levels), percentage state varied significantly as a function of dose ($F = 3.842$, df = 4,60, $p = 0.008$), with a significant interaction of state and dose ($F = 4.121$, df = 16,60, $p = 0.000$). Given the parallel changes in transitional states, subsequent ANOVAs were performed for W, for tSWS together with SWS, and for tPS together with PS (with state as a grouping factor). For all states, there was a significant main effect of dose, although the maximal trend, examined by polynomial contrasts, differed per state (wake with the linear polynomial: $F = 54.666$, df = 1,3, $p = 0.005$; tSWS, SWS with the linear: $F = 29.057$, df = 1,6, $p = 0.002$; and tPS, PS with the quadratic: $F = 24.073$, df = 1,6, 0.003; $^{**}p \leq 0.01$).

DISCUSSION

The results of the present study demonstrate that NT, which selectively binds to, internalizes within, and induces bursting of cholinergic basal forebrain neurons after local microinjection, diminishes δ activity with SWS and stimulates γ and θ activity with wake and PS states.

Visualization of the fluorescent analog, Fluo-NT, and recording of unit activity in ChAT-immunoreactive neurons both indicated here that NT injected into the basal forebrain targeted and directly altered the discharge of the cholinergic cells therein. After its microinjection, Fluo-NT was found to be selectively internalized within ChAT-immunoreactive neurons, reflecting its selective high-affinity binding to those cells (Faure et al., 1995). Moreover, juxtacellularly recorded and Nb-labeled, ChAT-immunoreactive neurons were found to increase their rate of firing and to discharge in bursts after the microinjection of NT here in anesthetized animals, similarly to the manner in which identified cholinergic neurons were shown to be directly modulated by NT in the slice (Alonso et al., 1994).

In the naturally waking–sleeping animals, NT microinjections promoted cortical activation, which was evident as a decrease in δ and an increase in γ activity during the day when the rats are normally in SWS the majority of the time. These EEG changes may be attributed to the release of ACh from terminals of the discharging cholinergic basalocortical neurons and postsynaptic action of ACh on cells in the cerebral cortex. ACh has been shown to depolarize pyramidal cells through long-acting muscarinic receptors that close K^+ channels and thus increase excitability and promote tonic firing in these cells (Krnjevic, 1967; McCormick and Prince, 1986; Metherate et al., 1992). Here, the increase in γ was antagonized by previous administration of atropine, the muscarinic

Table 3. EEG and state effects during the 30 min post-injection period after (0.25 mM) NT after previous systemic administration of atropine[a]

	Drug trials			
	Ringer's	(0.25 mM) NT	Atropine and (0.25 mM) NT	Statistic[a] (*F*)
Activity (Total)				
γ	114.3 ± 1.2	19.0 ± 0.3	14.1 ± 1.0	45.3*
δ	19.6 ± 2.2	14.4 ± 2.2	22.9 ± 0.9	37.3*
θ/δ	1.18 ± 0.09	1.42 ± 0.18	1.08 ± 0.02	4.90
EMG	269.8 ± 93.1	313.9 ± 67.0	323.2 ± 72.1	
State				
Wake	22.8 ± 6.5	41.8 ± 15.8	75.6 ± 24.4	
tSWS + SWS	62.2 ± 1.8	5.7 ± 4.6	14.8 ± 14.8	7.9*
tPS + PS	15.0 ± 5.0	52.5 ± 17.4	9.6 ± 9.6	11.9*

[a]Data are presented as mean ± SEM average values for 20 sec epochs for Ringer's, NT, and (30 mg/kg, i.p.) atropine and NT for repeated trials in three rats. For EEG activity, γ and δ are presented as relative amplitude (% total amplitude), together with θ/δ ratio and EMG absolute amplitude. For each variable, a repeated measures ANOVA was performed to test the *post hoc* hypothesis with orthogonal c-matrices that the effect of NT was reversed by atropine. Results are shown in those cases where Ringer's did not differ significantly from atropine and NT (with coefficients for Ringer's: −0.707; NT: 0; and atropine and NT: +0.707), and show the *F*-ratio for the c-matrix comparing NT on the one hand with Ringer's and atropine and NT on the other (with coefficients for Ringer's: −0.408, NT: +0.816, and atropine and NT: −0.408, where * indicates $p < 0.05$, df = 1,6). For % state, a repeated measures ANOVA was first performed across drug conditions (Ringer's, NT, or atropine and NT) with state (3) as a grouping factor and revealed a significant interaction of drug with state ($F = 7.69$, df = 4,12, $p = 0.003$). In *post hoc* tests using the orthogonal c-matrices for each state, it was found that wake after atropine and NT differed significantly from Ringer's ($F = 7.22$, $p = 0.036$, df = 1,6), and not (together with Ringer's) from NT ($F = 0.40$, df = 1,6). For tSWS + SWS and for tPS + PS, however, the difference between Ringer's and atropine and NT was not significant, whereas that between NT on the one hand and Ringer's and atropine and NT on the other was, as indicated.

antagonist, confirming the importance of cortical ACh release and postsynaptic action on muscarinic receptors for this EEG change after the NT injections.

In addition to an increase in γ activity, there was a marked increase in θ activity after NT microinjections into the basal forebrain. Induction of θ activity was also shown to occur in another study using intracerebroventricular administration of NT (Castel et al., 1989). The promotion of θ activity in both cases may be caused by the stimulation of rhythmic burst discharge of basalocortical cholinergic neurons and thus rhythmic release of ACh from their terminals in the cortex. Here, as in previous studies, the precise frequency of θ-like activity was found to differ across cortical leads and could not be attributed to a volume-conducted signal from the hippocampus or entorhinal cortex, as considered previously (Maloney et al., 1997). The peak frequency was highest on the retrosplenial cortical lead and lowest on the frontal lead, which is over the anterior medial or prefrontal cortex. It was shown previously that θ in the cingulate–retrosplenial cortex is generated there and persists after lesions of the medial septum (Borst et al., 1987; Leung and Borst, 1987), thus being independent of the septohippocampal system. These data strongly suggested that cingulate–retrosplenial θ is dependent on input from the basal forebrain. Indeed, it was found recently that identified cholinergic basal forebrain neurons discharge in rhythmic bursts in association with stimulation-induced θ-like activity from the retrosplenial and also prefrontal cortex in urethane-anesthetized rats (Manns et al., 2000), thus substantiating this possibility. Here, rhythmic bursting activity that was cross-correlated with rhythmic EEG activity was seen in Nb-labeled ChAT-immunoreactive neurons after NT microinjections. As had been found in the former study, it was also found in these units that the rhythmic bursting was at a higher frequency for the unit with a discharge that matched the predominant retrosplenial activity than for the unit with a discharge that matched the slower predominant prefrontal activity. These results suggest that bursting cholinergic neurons modulate cortical activity

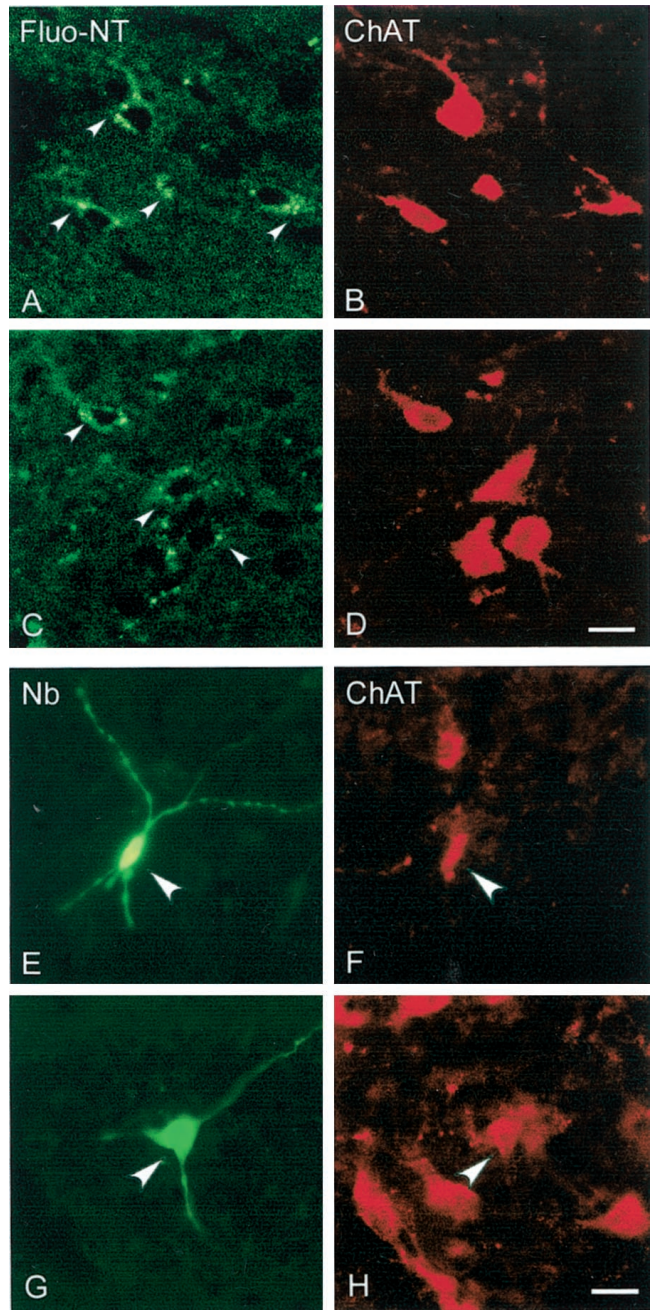

Figure 7. Photomicrographs showing fluorescent staining after Fluo-NT microinjections (*A–D*) and Nb juxtacellular application (*E*, *F*) in association with ChAT-immunostaining. When viewed under illumination for fluorescein (*A*, *C*), punctate fluorescent granules (*arrowheads*) were visible in the cytoplasm of perikarya and proximal dendrites of relatively large neurons, which when viewed under illumination for rhodamine were found to correspond to ChAT-immunoreactive cells (*B*, *D*). Neurons juxtacellularly recorded and labeled with Nb (revealed by green fluorescent Cy2-conjugated streptavidin) in the SI and MCPO (*E* and *F*, respectively; indicated by *stars* in Fig. 1) were identified as ChAT-immunoreactive (*G* and *H*; revealed by red fluorescent Cy3-conjugated secondary antibodies). Scale bar, 20 μm.

in a θ-like manner, with potentially different frequencies for different cortical areas during some behaviors yet with the possibility for coordinated discharge at similar frequencies during other behaviors and states. Accordingly, the θ activity measured on different cortical leads after NT microinjections in the freely moving, naturally waking–sleeping rats may be stimulated by rhythmically bursting cholinergic neurons projecting to different regions of the cerebral cortex and stimulating regionally particular or coordinated frequencies of θ-like activity during the resulting behavioral states.

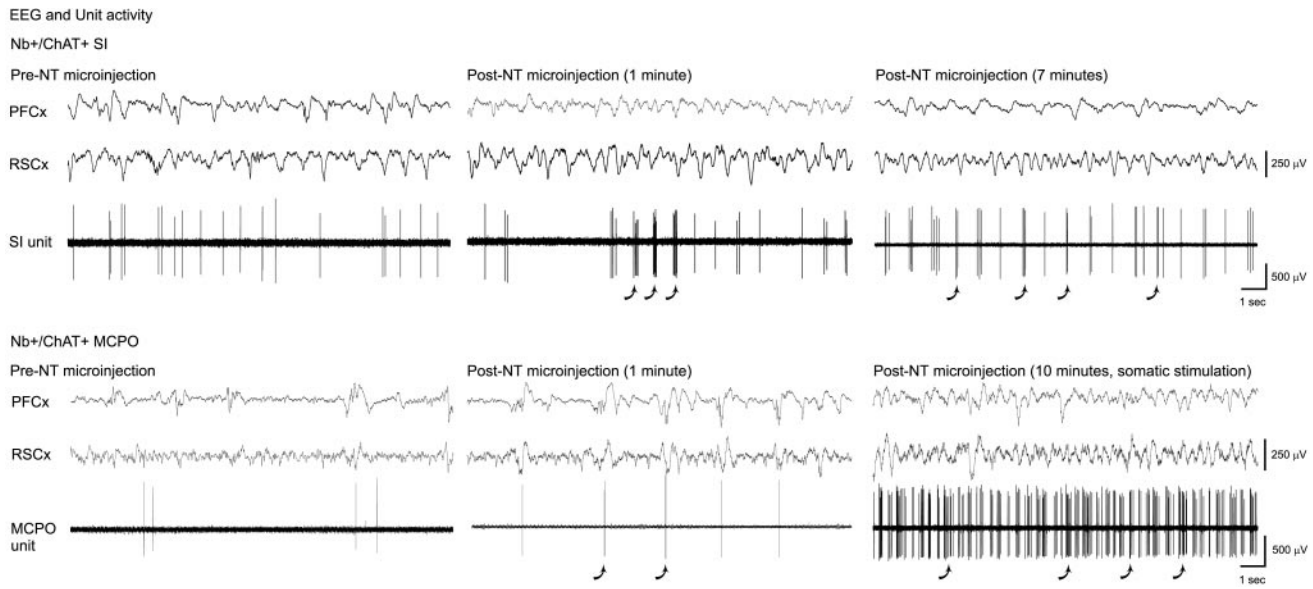

Figure 8. Discharge patterns of Nb+/ChAT+ neurons in SI (*top*; cell in Fig. 7*E*,*F*) and MCPO (*bottom*; cell in Fig. 7*G*,*H*) in association with NT unilateral microinjection in urethane-anesthetized animals. Presented are EEG activity from prefrontal (*PFCx*) and retrosplenial cortex (*RSCx*) and associated unit activity before, 1 min after, and several minutes after the NT microinjection. Note the change from a single spiking discharge to a burst discharge, in addition to an increased rate of discharge, after NT microinjection. This burst discharge takes on a rhythmic character in association with EEG activation after NT (spontaneously in SI unit and with somatic stimulation in MCPO unit). *Arrows* indicate examples of high-frequency bursts (>80 Hz and in some cases beyond resolution of the printing).

In contrast to the changes in γ and δ, the increase in the θ/δ ratio after NT microinjections was attenuated but not conclusively antagonized by atropine, because the change was not statistically significant. As noted here, however, atropine produces a dissociated state of behavioral waking with slow EEG activity, yet sometimes with θ activity when animals are moving (Vanderwolf, 1975). θ on the EEG after NT microinjections following atropine could represent such atropine-resistant θ occurring during active waking. Recent evidence has indicated that in addition to the cholinergic neurons, a small subset of noncholinergic neurons in the diagonal band–medial septum are modulated by NT *in vitro* (Matthews, 1999). It is possible that atropine-resistant θ may be stimulated by NT through direct action on such noncholinergic neurons, although such action was not found on the noncholinergic neurons sampled *in vitro* in the substantia innominata–magnocellular preoptic region (Alonso et al., 1994). θ in the cortex as in the hippocampus may depend on noncholinergic, in addition to cholinergic, neurons (Lee et al., 1994). Here after NT microinjections, noncholinergic neurons could also be activated secondarily by local projections of the cholinergic neurons in the basal forebrain. In the presence of atropine, cholinergic transmission through local and distant projections would depend on nicotinic receptors. Atropine-resistant θ in the cortex could be stimulated by ACh released from rhythmically discharging cholinergic neurons by being transmitted through nicotinic receptors that have been shown to be located on interneurons (Xiang et al., 1998; Porter et al., 1999). Indeed, fast-acting, nicotinic receptors could be important in the temporally punctuated modulation of cortical activity that must occur with a θ-like frequency (Manns et al., 2000). Nonetheless, slower depolarization through muscarinic receptors can also bring cortical neurons within the optimal subthreshold range in which they can oscillate at a θ frequency (Klink and Alonso, 1993), and faster depolarization of interneurons through muscarinic receptors (McCormick and Prince, 1986) could further shape the oscillations at this frequency. Here, the most prominent θ that occurred with enhanced PS and tPS after NT was fully antagonized by atropine, indicating the importance of both the cholinergic neurons and muscarinic receptors in this response to NT.

The changes induced by NT in cortical activity were also associated with remarkable changes in sleep–wake states. First, SWS was diminished in a dose-dependent manner by the NT microinjections during the time of day when the rats are normally in SWS the majority of the time. Wake was reciprocally increased. Yet, it was a quiet wake state with low EMG and often marked by a reclining, normally sleeping posture with eyes open. During this quiet waking behavioral state, θ activity was present on the EEG, an association rarely if ever seen in the normal rat (Maloney et al., 1997), in which, as documented for hippocampal θ (Vanderwolf, 1975), cortical θ-like activity accompanies moving or attentive behaviors. The θ that was stimulated by NMDA injections into the basal forebrain was associated, as in the normal rat, with an active moving waking state and high EMG (Cape and Jones, 2000), but NMDA would also be associated with stimulation of multiple cell types in the basal forebrain, thus stimulating the high EMG activity along with cortical activation. Here, NT microinjections were not associated with an increase in EMG activity, perhaps because of the selective activation of the cholinergic neurons along with their target neurons, which must also occur during natural PS with muscle atonia. Indeed, NT microinjections lead to a dose-dependent increase in PS and the tPS in the absence of SWS. This extraordinary induction of θ EEG activity associated with the occurrence and enhancement of narcoleptic-like PS may be produced by rhythmic bursting discharge of cholinergic neurons without the participation of those noncholinergic basal forebrain neurons having ascending and/or descending projections that are recruited by additional afferents during active waking.

From the present results, NT would appear to have a potent capacity to modulate both cortical activity and sleep–wake state through its unique action on basal forebrain cholinergic neurons. Whether NT exerts this potential in the natural state could not be tested here because of the lack of an appropriate water-soluble antagonist of NT that could be injected into the basal forebrain. NT is contained in basal forebrain afferents that originate in both brainstem and forebrain (Morin and Beaudet, 1998), including neurons in the posterior hypothalamus, from which θ can be elicited by electrical stimulation (Bland and Vanderwolf, 1972). In any event, its unique action in the basal forebrain reveals the extraordinary capacity of the cholinergic neurons to stimulate cortical activation with rhythmic θ and γ independent of motor activity and to promote the state of PS. It is perhaps during such cholinergically stimulated rhythmic modulation, and thus during PS in addition to waking, that plasticity

as well as coherence may be maximized in neocortical, as in hippocampal, networks (Huerta and Lisman, 1993; Winson, 1993; Jones, 1998; Manns et al., 2000).

REFERENCES

Alonso A, Faure M-P, Beaudet A (1994) Neurotensin promotes oscillatory bursting behavior and is internalized in basal forebrain cholinergic neurons. J Neurosci 14:5778–5792.

Bland BH, Vanderwolf CH (1972) Diencephalic and hippocampal mechanisms of motor activity in the rat: effects of posterior hypothalamic stimulation on behavior and hippocampal slow wave activity. Brain Res 43:67–88.

Borst JGG, Leung L-WS, MacFabe DF (1987) Electrical activity of the cingulate cortex. II. Cholinergic modulation. Brain Res 407:81–93.

Cape EG, Jones BE (1998) Differential modulation of high frequency γ electroencephalogram activity and sleep–wake state by noradrenaline and serotonin microinjections into the region of cholinergic basalis neurons. J Neurosci 18:2653–2666.

Cape EG, Jones BE (2000) Effects of glutamate agonist versus procaine microinjections into the basal forebrain cholinergic cell area upon gamma and theta EEG activity and sleep-wake state. Eur J Neurosci 12:2166–2184.

Casamenti F, Deffenu G, Abbamondi AL, Pepeu G (1986) Changes in cortical acetylcholine output induced by modulation of the nucleus basalis. Brain Res Bull 16:689–695.

Castel M-N, Stutzmann J-M, Lucas M, Lafforgue J, Blanchard J-C (1989) Effects of ICV administration of neurotensin and analogs on EEG in rats. Peptides 10:95–101.

Celesia GG, Jasper HH (1966) Acetylcholine released from cerebral cortex in relation to state of activation. Neurology 16:1053–1064.

Faure M-P, Alonso A, Nouel D, Gaudriault G, Dennis M, Vincent J-P, Beaudet A (1995) Somatodendritic internalization and perinuclear targeting of neurotensin in the mammalian brain. J Neurosci 15:4140–4147.

Gritti I, Mainville L, Jones BE (1994) Projections of GABAergic and cholinergic basal forebrain and GABAergic preoptic-anterior hypothalamic neurons to the posterior lateral hypothalamus of the rat. J Comp Neurol 339:251–268.

Gritti I, Mainville L, Mancia M, Jones BE (1997) GABAergic and other non-cholinergic basal forebrain neurons project together with cholinergic neurons to meso- and iso-cortex in the rat. J Comp Neurol 383:163–177.

Huerta PT, Lisman JE (1993) Heightened synaptic plasticity of hippocampal CA1 neurons during a cholinergically induced rhythmic state. Nature 364:723–725.

Jasper HH, Tessier J (1971) Acetylcholine liberation from cerebral cortex during paradoxical (REM) sleep. Science 172:601–602.

Jones BE (1998) The neural basis of consciousness across the sleep-waking cycle. Consciousness: at the frontiers of neuroscience, advances in neurology (Jasper HH, Descarries L, Castellucci VF, Rossignol S, eds), pp 75–94. Philadelphia: Lippincott-Raven.

Khateb A, Muhlethaler M, Alonso A, Serafin M, Mainville L, Jones BE (1992) Cholinergic nucleus basalis neurons display the capacity for rhythmic bursting activity mediated by low threshold calcium spikes. Neuroscience 51:489–494.

Khateb A, Fort P, Serafin M, Jones BE, Muhlethaler M (1995) Rhythmical bursts induced by NMDA in cholinergic nucleus basalis neurones *in vitro*. J Physiol (Lond) 487.3:623–638.

Klink R, Alonso A (1993) Ionic mechanisms for the subthreshold oscillations and differential electroresponsiveness of medial entorhinal cortex layer II neurons. J Neurophysiol 70:144–157.

Krnjevic K (1967) Chemical transmission and cortical arousal. Anesthesiology 28:100–104.

Lee MG, Chrobak JJ, Sik A, Wiley RG, Buzsaki G (1994) Hippocampal theta activity following selective lesion of the septal cholinergic system. Neuroscience 62:1033–1047.

Lehmann J, Nagy JI, Atmadja S, Fibiger HC (1980) The nucleus basalis magnocellularis: the origin of a cholinergic projection to the neocortex of the rat. Neuroscience 5:1161–1174.

Leung L-WS, Borst JGG (1987) Electrical activity of the cingulate cortex. I. Generating mechanisms and relations to behavior. Brain Res 407:68–80.

LoConte G, Casamenti F, Bigi V, Milaneschi E, Pepeu G (1982) Effect of magnocellular forebrain nuclei lesions on acetylcholine output from the cerebral cortex, electrocorticogram and behaviour. Arch Ital Biol 120:176–188.

Maloney KJ, Cape EG, Gotman J, Jones BE (1997) High frequency gamma electroencephalogram activity in association with sleep-wake states and spontaneous behaviors in the rat. Neuroscience 76:541–555.

Manns ID, Alonso A, Jones BE (2000) Discharge properties of juxtacellularly labeled and immunohistochemically identified cholinergic basal forebrain neurons recorded in association with the electroencephalogram in anesthetized rats. J Neurosci 20:1505–1518.

Matthews RT (1999) Neurotensin depolarizes cholinergic and a subset of non-cholinergic septal/diagonal band neurons by stimulating neurotensin-1 receptors. Neuroscience 94:775–783.

McCormick DA, Prince DA (1986) Mechanisms of action of acetylcholine in the guinea-pig cerebral cortex in vitro. J Physiol (Lond) 375:169–194.

Metherate R, Cox CL, Ashe JH (1992) Cellular bases of neocortical activation: modulation of neural oscillations by the nucleus basalis and endogenous acetylcholine. J Neurosci 12:4701–4711.

Morin AJ, Beaudet A (1998) Origin of the neurotensinergic innervation of the rat basal forebrain studied by retrograde transport of cholera toxin. J Comp Neurol 391:30–41.

Morin AJ, Tajani M, Jones BE, Beaudet A (1996) Spatial relationship between neurotensinergic axons and cholinergic neurons in the rat basal forebrain: a light microscopic study with three-dimensional reconstruction. J Chem Neuroanat 10:147–156.

Pinault D (1996) A novel single-cell staining procedure performed in vivo under electrophysiological control: morpho-functional features of juxtacellularly labeled thalamic cells and other central neurons with biocytin or Neurobiotin. J Neurosci Methods 65:113–136.

Porter JT, Cauli B, Tsuzuki K, Lambolez B, Rossier J, Audinat E (1999) Selective excitation of subtypes of neocortical interneurons by nicotinic receptors. J Neurosci 19:5228–5235.

Rye DB, Wainer BH, Mesulam M-M, Mufson EJ, Saper CB (1984) Cortical projections arising from the basal forebrain: a study of cholinergic and noncholinergic components employing combined retrograde tracing and immunohistochemical localization of choline acetyltransferase. Neuroscience 13:627–643.

Szigethy E, Beaudet A (1987) Selective association of neurotensin receptors with cholinergic neurons in the rat basal forebrain. Neurosci Lett 83:47–52.

Szigethy E, Leonard K, Beaudet A (1990) Ultrastructural localization of [^{125}I]neurotensin binding sites to cholinergic neurons of the rat nucleus basalis magnocellularis. Neuroscience 36:377–391.

Vanderwolf CH (1975) Neocortical and hippocampal activation in relation to behavior: effects of atropine, eserine, phenothiazines and amphetamine. J Comp Physiol Psychol 88:300–323.

Winson J (1993) The biology and function of rapid eye movement sleep. Curr Opin Neurobiol 3:243–248.

Xiang Z, Huguenard JR, Prince DA (1998) Cholinergic switching within neocortical inhibitory networks. Science 5379:985–988.